· Article ·
doi: 10.13679/j.advps.2015.3.00256

Advances in Polar Science
September 2015 Vol. 26 No. 3: 256-263

Observations of stratospheric ozone above Ny-Ålesund in the Arctic, 2010–2011

LUO Yuhan[1]*, SI Fuqi[1], LIU Wenqing[1], SUN Liguang[2] & LIU Yi[3]

[1] Anhui Institute of Optics & Fine Mechanics, Chinese Academy of Sciences, Hefei 230031, China;

[2] Institute of Polar Environment, School of Earth and Space Sciences, University of Science and Technology of China, Hefei 230026, China;

[3] National Synchrotron Radiation Laboratory, University of Science and Technology of China, Hefei 230029, China

Received 16 June 2015; accepted 17 September 2015

Abstract Stratosphere ozone depletion above the Arctic region has drawn increased attention recently. Here we present stratospheric ozone column densities above Ny-Ålesund in the Arctic during summer 2010 and 2011, based on a self-developed passive differential optical absorption spectroscopy (DOAS) technique. By analyzing the received scattered solar spectrum, daily variations of ozone vertical column densities (VCDs) were obtained and correlated with satellite-borne ozone monitoring results and ozone sonde data. The comparisons showed good correlation, confirming the feasibility of DOAS in high-latitude Arctic regions. The preliminary analysis also demonstrated that abnormal low-level ozone columns found in spring 2011 had negative impacts on total ozone column densities over the entire year. The loss of stratospheric ozone may be correlated with low stratospheric temperatures, where heterogeneous atmospheric reactions were active.

Keywords ozone, Arctic, DOAS

Citation: Luo Y H, Si F Q, Liu W Q, et al. Observations of stratospheric ozone above Ny-Ålesund in the Arctic, 2010–2011. Adv Polar Sci, 2015, 26: 256-263, doi: 10.13679/j.advps.2015.3.00256

1 Introduction

Ozone depletion events and their environmental effects have received substantial attention for some time. Since discovery of the ozone hole over the Antarctic in the 1980s, ozone column densities continued to decrease with fluctuation and reached a minimum during 1992–1993[1]. As anthropogenic emission of chlorofluorocarbons (CFCs) and corresponding halogen compounds have increased in the stratosphere, the Antarctic ozone hole has worsened, combined with atmospheric dynamics and photochemical processes[2]. In recent years, as CFCs were gradually degrading the atmosphere and the Antarctic stratosphere warmed with the pace of global warming, the Antarctic ozone hole appeared to have a shrinking trend[3-6].

However, some low-ozone areas and tiny ozone holes have been found in the Northern Hemisphere, e.g., over the Qinghai–Tibetan plateau during winter since 1995[7]. Such phenomena have also occurred over Europe[8]. At the end of March 2011, the most severe and largest ozone losses were recorded over the Arctic, by both satellite-borne instrumentation and ground-based observation networks[9-13]. During this breaking ozone depletion event, the total ozone column was as low as 220 DU) (which has been considered the ozone hole threshold for the Antarctic (1 DU= 2.668×10^{16} molec·cm^{-2}) in some areas. The ozone loss area reached nearly 70% of the Arctic area, which normally has the maximum column density of ozone during the aforesaid time.

The appearance of the ozone hole and unprecedented

* Corresponding author (email: yhluo@aiofm.ac.cn)

low ozone level over the Arctic would have a direct influence on ultraviolet-B (UV-B) radiation at the earth surface, which is harmful to the eco-environment. Therefore, it is of great importance to determine changes in total ozone level, especially over North Hemisphere.

Balloon-borne measurements were first made at the Arctic's Ny-Ålesund research station in 1991. The results showed that ozone depletion is related to low temperature in the stratosphere, which facilitates polar stratospheric cloud (PSC) formation over long periods[14]. Rex et al.[15] also reported that Arctic ozone will decrease by ~15 DU with a stratospheric temperature decrease of 1 K.

The ground-based total ozone detection was mainly based on a dual (multi) wavelength technique, e.g., Dobson and Brewer spectrophotometer. From the 1980s, the differential optical absorption spectroscopy (DOAS) method has been used to derive atmospheric columns for a number of important trace species, including total ozone, nitrogen dioxide, and bromine oxide[16]. According to characteristic absorption cross sections at different wavelengths and absorption intensities, trace gases can be identified and measured[17-21]. Using this method, we reported tropospheric NO_2 results from 2011 and evaluated sources of ship emissions[22].

Here, we present total ozone column densities at Ny-Ålesund using ground-based passive DOAS. Daily variations of ozone column densities were retrieved and compared with satellite Ozone Monitoring Instrument (OMI) data (discussed in Section 2.6). Based on the preliminary results, we compare the ozone columns before and after the low ozone event in spring 2011 and discuss the possible reasons and regional influences.

2 Experiments and data analysis

2.1 Experimental site

Located on the west coast of the Svalbard Islands and north end of the North Atlantic Warm Current (NAWC), Ny-Ålesund has a typical Arctic oceanic climate with very low temperature at high altitude and relatively high temperature near sea level. Influenced by the NAWC, the weather changes frequently because of the character of the frigid oceanic climate. As a result, atmospheric circulation and exchange at elevation is stronger than at other locations at the same latitude, which is a unique character of the research site. This site is in an abandoned Norwegian mining area and has become an international research community with no local industry nearby.

The instrument was established at Zeppelin Station of Ny-Ålesund (78°54′26″N, 11°53′9″E, 474 m a.s.l.) from 14 July to 26 August 2010 and 6 July to 16 August 2011. A schematic view of the observation location and instrument is shown in Figure 1. Given the limited solar zenith angle (SZA) range at other times of the year, we chose the two summer periods above for observation, which have comparatively longer sunshine and smaller solar zenith angles.

2.2 Ground-based DOAS setup

The DOAS instrument was used to obtain ozone column densities. We observed electronic transitions of the trace gas molecules (or atoms) in the ultraviolet and visible wavelength ranges. Like the other absorption spectroscopic techniques, DOAS uses characteristic absorption features of

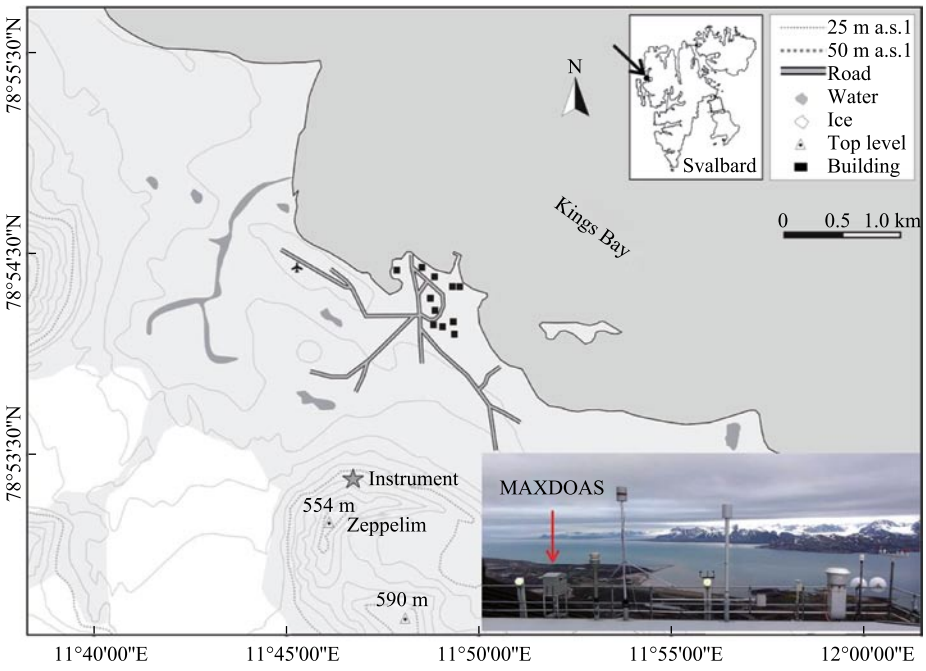

Figure 1 Schematic view of experiment.

trace gas molecules along the detected light path in the open atmosphere, thereby measuring atmospheric trace gases. Zenith-scattered DOAS is mostly used to detect those gases in the stratosphere, whereas off-axis DOAS is sensitive to boundary layer species.

The spectrometer collects zenith-scattered sunlight, which is dispersed by grating spectrographs (MAYA2000 Pro, Ocean Optics) and detected by an ILX511 linear array CCD. The incoming light is transformed by a quartz fiber (NA = 0.22) and detected by 2068 pixels (2048 in practice, with each unit 14 μm ×200 μm). The wavelength range is 290 to 420 nm. The entrance slit width is 100 μm, and spectral resolution 0.3 nm (0.6 nm for 2010). The detectors are thermally stabilized at ~10°C using a thermal controller. A computer sets the system configuration and controls the automatic measurements. Calibration measurements of dark current, offset and mercury lamp spectra were performed before the experiment.

The telescope was pointed north, which is least affected by direct sunlight. The reason is that when looking toward the sun, in particular for higher elevation angles, the air mass factor (AMF) is significantly smaller. This factor is a result of the strong forward peak in Mie scattering, which reduces the effective light path in such geometry. Only zenith-direction measurements were used in the research.

2.3 Data analysis

Spectra measured with the setup described above were analyzed using the DOAS retrieval method. Ozone differential slant column density (dSCD) was retrieved for 338–348 nm. O_3 (202 K), NO_2 (293 K), O_4 (298 K) and ring structure are involved in the inversion algorithm. High-resolution cross sections were convoluted with the instrument slit function, determined by measuring the emission line of a mercury lamp. A fifth-order polynomial was used to eliminate broad band structures in the spectra caused by Rayleigh and Mie scattering. Furthermore, a nonlinear intensity offset was included in the fit, to account for possible instrumental stray light. A wavelength shift and stretch of the spectra was allowed for in the fit to compensate for small changes in spectral adjustment of the spectrograph. Wavelength calibration was performed using WinDOAS software[23] by fitting the reference spectrum to a high-resolution Fraunhofer spectrum.

Taking the retrieved spectrum from 15 July 2010 as an example (Figure 2), the zenith sky spectrum at noon was used as the Fraunhofer reference spectrum (S_{FRS}).

Because anthropogenic ozone pollution is almost nonexistent in the study area, more than 90% of ozone is concentrated in the stratosphere. Thus, ozone vertical column

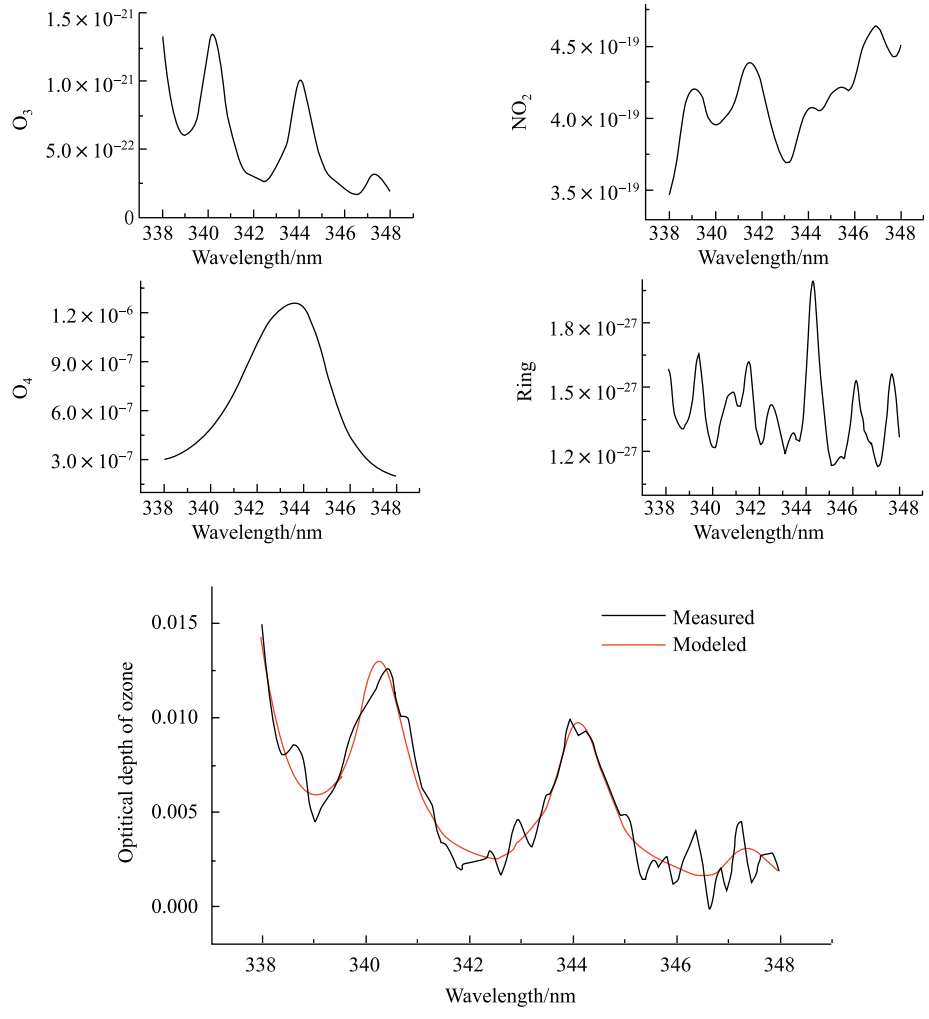

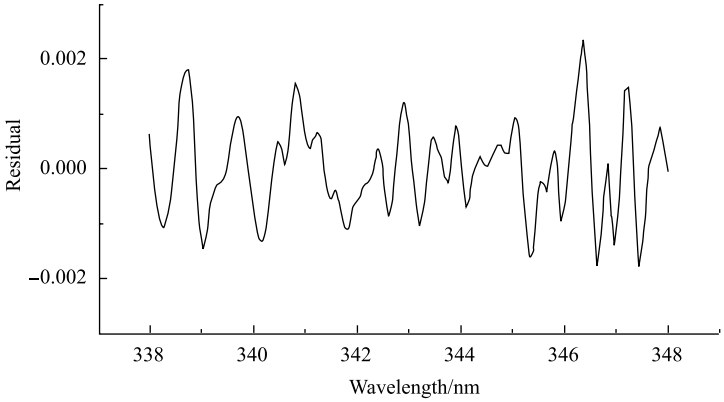

Figure 2 Cross sections of O_3, NO_2, O_4, ring, and an example of ozone fitting.

density is approximately constant over a half day (am/pm). Therefore, ozone column densities can be calculated by the following equation, in which S_{FRS} is the intercept and vertical column density (VCD) is the slope:

$$dSCD(\theta) = AMF(\theta) \times VCD - S_{FRS}.$$

AMF is calculated by the radiative transfer SCIATRAN model[24]. Ozone VCDs were retrieved by corresponding dSCDs and AMFs. Taking data from 17 July 2010 as an example, the linear fit of ozone dSCD and AMF is shown in Figure 3. The ozone VCD is 8.116×10^{18} molec·cm^{-2}, with a strong linear relationship between dSCD and AMF.

Uncertainties in the results are from uncertainties in the determination of dSCD, errors in the radiation transport model calculation, and the presence of clouds. For the first two, the error is on the order of 10% or less. For the influence of clouds, we avoided this source of error by selecting cloud-free periods using a cloud index retrieved by our system[25].

2.4 Meteorological parameters

Monthly-mean temperature profiles with altitude (atmospheric pressure) during the observation period at Ny-Ålesund were constructed using European Center for Mediumrange Weather Forecasts (ECMWF) ERA Interim reanalysis data (http://apps.ecmwf.int/datasets/data/interim-full-daily/levtype=pl) (Figure 4). This figure shows stratospheric temperature, and the altitude of the tropopause is clearly evident. We chose the temperature at the inversion layer near 250 mb as stratospheric temperature (Figure 5). We found that this temperature fluctuated almost every day and could change more than 20 degrees in a very short period.

2.5 Ozonesonde

The total ozone column and vertical profile have been recorded by the Alfred Wegener Institute using a balloon-borne ozonesonde since 1992. Total column ozone in DU is calculated by integrating the ozone partial pressure profile up to balloon-burst altitude and adding a residual amount, which is based on climatological ozone tables accounting for ozone above that altitude. Data frequency is approximately once per week, which provides profiles of temperature, pressure and ozone that can be used as input to the radiative transfer model. Ozone profiles during the observation periods are shown in Figure 6.

Polar ozonesonde profiles provide detailed vertical measurements of ozone that can be made even during dark

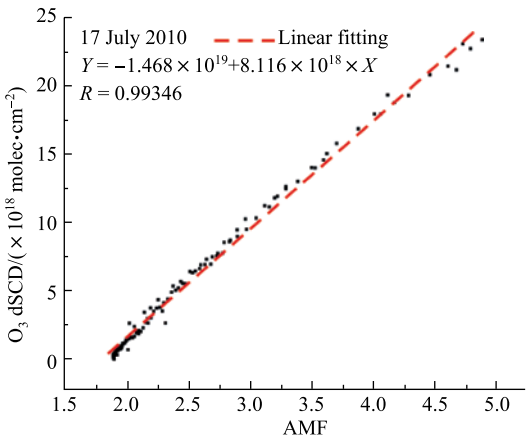

Figure 3 An example of linear fit of O_3 dSCD to AMF for 17 July 2010 (solar zenith angle is < 75°; noon spectrum is selected as FRS).

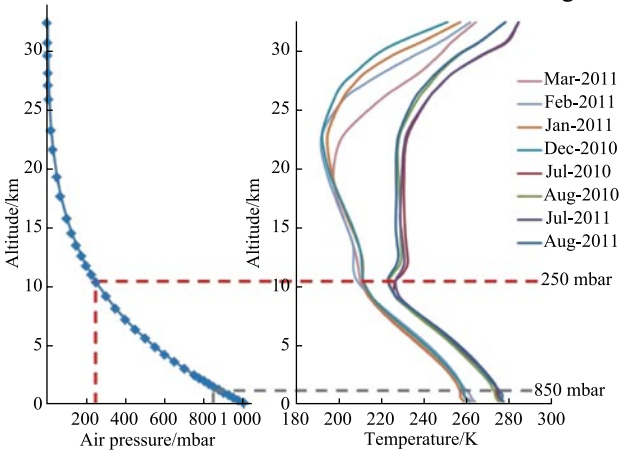

Figure 4 Monthly-mean temperature profiles with altitude (air pressure) during ozone loss period (data from ECMWF reanalysis: http://apps.ecmwf.int/datasets/data/interim-full-daily/levtype=pl).

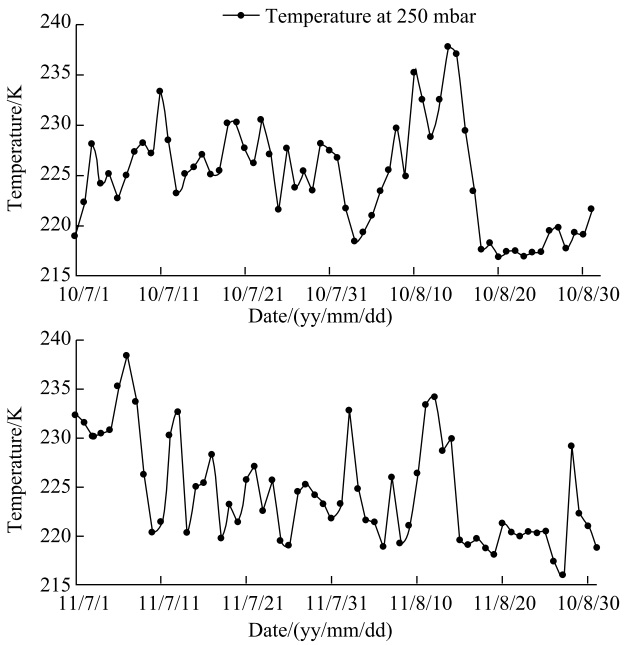

Figure 5 Temperature at 250-mb pressure level during the observation period (data from ECMWF reanalysis: http://apps.ecmwf.int/datasets/data/interim-full-daily/levtype=pl).

periods, when satellite ozone observations are limited. Therefore, the ozonesonde data can be effective validation for ground-based DOAS results.

2.6 Total Ozone Columns derived from OMI satellite observations

The OMI onboard NASA's EOS-AURA satellite measures multiple key species in stratospheric and tropospheric chemistry of the earth's atmosphere and for climate research. It is a nadir remote sensor that measures solar radiation backscattered by the atmosphere and surface over the entire wavelength range 270–500 nm, with spectral resolution ~0.5 nm, very high spatial resolution (13 km × 24 km) and daily global coverage.

To confirm the quality of satellite data products (http://toms.gsfc.nasa.gov), independent and well-calibrated reference measurements from ground-based DOAS systems were used as validation for the satellite data. The ozone columns reported here are also compared with OMI data (Sect. 3).

3 Results and discussion

3.1 Results

Based on the above setup, valid data from Zeppelin Station were preliminarily analyzed. Ozone VCD calculated by DOAS measurement and that from OMI and ozonesonde data are shown in Figure 7. For both ground-based and satellite-borne instruments, the total ozone columns presented similar trends during the two observation periods (2010 and 2011 summer).

From 14 July to 26 August 2010, the mean of ozone VCD by DOAS was 300.5 DU with maximum 342.0 DU and minimum 236.6 DU. From 6 July to 16 August 2011, the mean ozone VCD was 291 DU with maximum 338.5 DU and minimum 260.8 DU.

The total ozone VCDs fluctuated with the same pattern as stratospheric temperature. This correlation can be explained as follows. When the stratosphere becomes cold, PSCs form within the circumpolar vortex. These are composed of crystals and hydrated species of nitric acid and sulfuric acid. The active halogen species (Cl and Br) can participate in a heterogeneous chemical reaction cycle on PSC surfaces, thereby depleting stratospheric ozone. This process is more effective in cold conditions[26], and can even cause loss of ozone during summer. Thus, the total ozone VCDs had a decreasing trend. While when the stratosphere warms, the

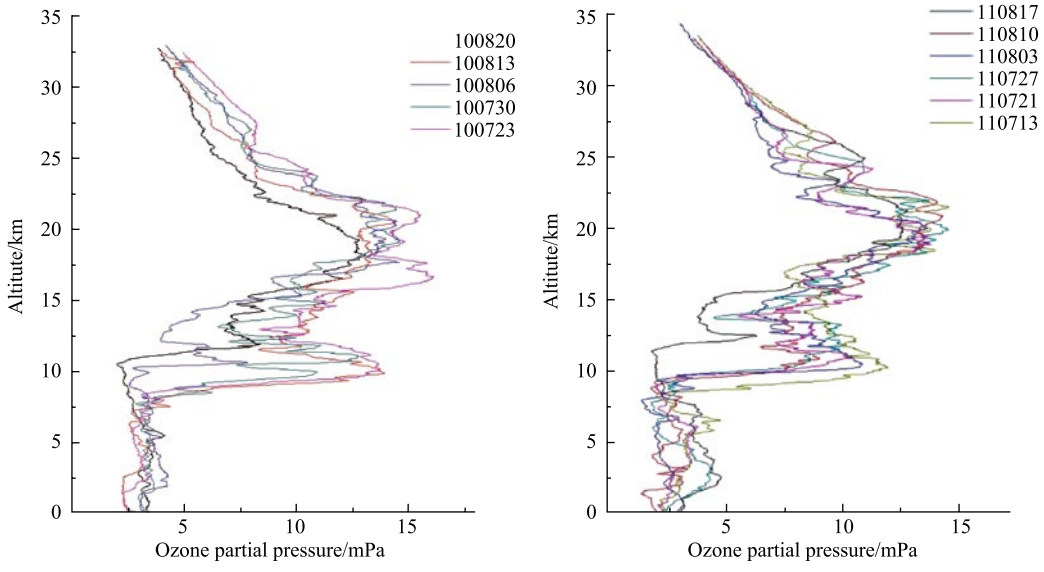

Figure 6 Ozone profile observed by ozonesonde at Ny-Ålesund in 2010 and 2011 summer (data from NDACC).

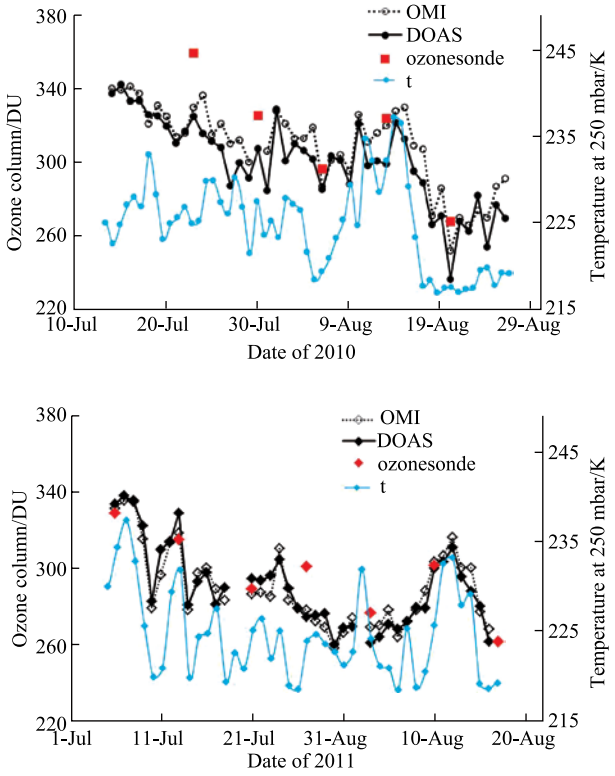

Figure 7 Total ozone VCDs observed by ground-based DOAS (black lines with solid dots), satellite-borne OMI (dashed lines with open dots), ozonesonde data (red dots), and stratospheric temperature (blue lines with blue solid dots) over Ny-Ålesund in 2010 (upper panel) and 2011 (lower panel) summers.

ozone loss cycle terminates with the disappearance of PSCs. As a result, the total ozone level has a transient recovery. If there is a persistent decline of temperature, it would be easier to find severe ozone depletion (e.g., 14 to 20 August 2010 and 7 to 10 July 2011).

3.2 Validation

To validate the accuracy of the ground-based DOAS observation of total ozone, satellite-borne OMI overpass data were compared with DOAS results. As shown in Figure 8, total ozone VCDs in summer 2010 and 2011 from ground-based DOAS and satellite-borne OMI observations have a linear fit. The DOAS and OMI measurements of total column ozone in 2010 and 2011 have a large correlation coefficient (R^2), 0.88356 and 0.91456, respectively. This confirms that the DOAS technique is effective in measuring ozone in the Arctic region.

Integrating the results of total ozone column from the passive DOAS and OMI shows a certain deviation, which was caused by the different observation pattern. For ground-based DOAS measurements, stratospheric ozone VCD is mainly determined from measurements at high SZA, which have the greatest influence on the Langley plot. For high SZA, light paths through the stratosphere become extremely long (up to several hundred kilometers). The OMI was pointed in the nadir direction, reflecting the overpass value (normally at noon, which are made at smaller SZA) of the pixel (13× 24 km^2). Thus, the DOAS probably has a larger footprint than the OMI observations. Thereby, for a given location, the ground-based DOAS and satellite OMI observation have different spatial and temporal accuracies for trace gas column densities. Further, on cloudy days, absorbers above cloud would be obscured from ground-based instruments. Thus, for stratospheric gases like ozone, the total columns are easily underestimated, which was another the reason why ozone VCDs by DOAS were slightly lower than those from OMI.

The ozonesonde data also had trends similar to the DOAS results (Figure 7). However, because the ozonesonde is influenced by the wind profile, the balloon could not be located at the same latitude and longitude during the monitoring period. Therefore, the results could either overestimate (e.g., 27 July 2011) or underestimate (e.g., 13 July 2011) the true column at the observation site.

3.3 Trends of Arctic ozone column variation

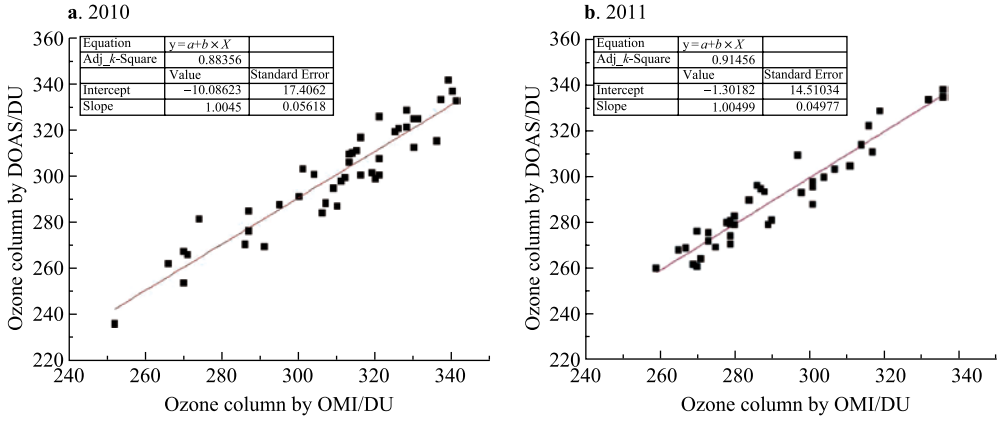

Figure 8 Comparisons of ozone column densities by passive DOAS and OMI measurement (data from http://toms.gsfc.nasa.gov) during observation at Zeppelin Station, Arctic.

Overpass ozone VCDs at Ny-Ålesund, Arctic from 2005 to 2011 (days 60–120) are displayed in Figure 9. Averages for 2005–2010 and data of 2011 are plotted separately. The natural seasonal cycle of total ozone over the Arctic shows large values in spring, as a result of increased transport of ozone from the tropics (source region) toward the polar regions in winter. However, there was a different pattern from March to mid-April 2011 (red solid dots) in that a severe ozone loss was observed by both satellite and ground-based instruments.

To address the hypothesis that ozone destruction somewhat depends on stratospheric temperature, Figure 10 illustrates stratospheric temperature (at the 250-mb pressure level) variation in the same period as Figure 9. We find that the total ozone columns changed synchronously with stratospheric temperature. Stratospheric temperature in 2011 (red solid dots) was much colder than in other years during all of March. This temperature declined dramatically to ~200 K (−70°C), which was about the level of Antarctic PSCs.

In the Arctic, total ozone variations are different from those observed in the Antarctic. The differences are normally attributed to atmospheric circulations and temperature variations. Unlike the Antarctic polar vortex, which isolates air inside it and has a very low temperature, dynamic atmospheric exchanges in the Arctic region are much more frequent. In particular for the Ny-Ålesund area, the North Atlantic Drift brings in water vapor continuously and there is

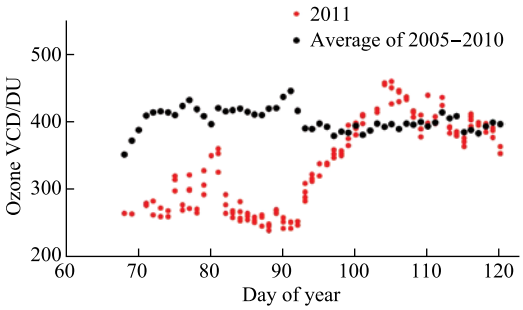

Figure 9 Overpass ozone VCDs at Ny-Ålesund, Arctic from 2005 to 2011 (days 60–120). Red dots are data of 2011, black dots are averages of 2005–2010 (data from http://avdc.gsfc.nasa.gov).

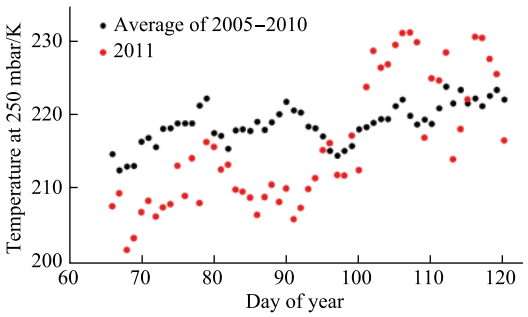

Figure 10 Stratospheric temperature (at 250-mb level) at Ny-Ålesund, Arctic from 2005 to 2011 (days 60–120). Red dots are data of 2011, black dots are averages 2005–2010 (data from ECMWF reanalysis).

vertical exchange with the tropopause. Moreover, exchanges at high latitude between northern Eurasia and northern Canada may also generate turbulence.

Therefore, it is assumed that significant Arctic ozone layer depletion can form in the case of a cold and stable Arctic stratosphere during winter. Stratospheric ozone depletion occurs over the polar regions when temperatures drop and PSCs form in the stratosphere. Chemical reactions that convert innocuous reservoir gases (e.g., hydrochloric acid) into active ozone-depleting gases take place on the surface of PSC particles, which can lead to rapid destruction of ozone as sunlight appears in spring. By comparing the ozone columns with stratospheric temperature, we have confirmed this assumption.

4 Conclusions

Ozone column densities at Ny-Ålesund in the Arctic were detected based on a ground-based DOAS technique. By comparing with satellite-borne OMI overpass and ozonesonde data, it was confirmed that DOAS is a promising tool for automatically and continuously observing the total ozone column at Arctic high latitudes.

The influence of stratospheric temperature on total column ozone was discussed. The decrease of stratospheric temperature can deplete total ozone at temperatures even higher than 220 K during summer. Trends of Arctic ozone columns from 2005 to 2011 spring (days 60–120) were illustrated and evaluated. A possible reason for the low ozone level in 2011 was also believed strongly related to low stratospheric temperature during March. The Arctic ozone depletion mechanism is still under research, and more data needed for its analysis.

Acknowledgements This research was financially supported by the Natural Science Foundation of China (Grant no. 41306199) and the Dean Research Funds for CAS Hefei Institute (Grant no. YZJJ201304). We are grateful to the Chinese Antarctic and Arctic Administration and teammates of the 2010 and 2011 Chinese Arctic Yellow River Station expeditions. We kindly acknowledge the Alfred-Wegener-Institute, Norwegian Polar Institute, and in particular the Norwegian Institute for Air Research (NILU).

References

1 Solomon S. Stratospheric ozone depletion: A review of concepts and history. Rev Geophys, 1999, 37(3): 275–316
2 Rowland F S. Stratospheric ozone depletion. Phil Trans R Soc B, 2006, 361(1469): 769–790
3 Grooß J U, Brautzsch K, Pommrich R, et al. Stratospheric ozone chemistry in the Antarctic: what determines the lowest ozone values reached and their recovery? Atmos Chem Phys, 2011, 11(23): 12217–12226
4 Bodeker G E, Shiona H, Eskes H, et al. Indicators of Antarctic ozone depletion. Atmos Chem Phys, 2005, 5(10): 2603–2615
5 Kerr R A. First detection of ozone hole recovery claimed. Science, 2011, 332(6026): 160
6 Hu Y Y, Xia Y, Gao M, et al. Stratospheric temperature changes and

ozone recovery in the 21st Century. Acta Meteorol Sin, 2009, 23(3): 263–275
7 Zou H. Seasonal variation and trends of TOMS ozone over Tibet. Geophys Res Lett, 1996, 23(9): 1029–1032
8 Allaart M, Valks P, van der A R, et al. ozone mini-hole observed over Europe, influence of low stratospheric temperature on observations. Geophys Res Lett, 2000, 27(24): 4089–4092.
9 Liu N Q, Huang F X, Wang W H. Monitoring of the 2011 Spring low ozone events in the Arctic region. Chin Sci Bull, 2011, 56(27): 2893–2896, doi: 10.1007/s11434-011-4636-3 (in Chinese)
10 Sinnhuber B M, Stiller G, Ruhnke R, et al. Arctic winter 2010/2011 at the brink of an ozone hole. Geophys Res Lett, 2011, 38(24): L24814
11 Manney G L, Santee M L, Rex M, et al. Unprecedented Arctic ozone loss in 2011. Nature, 2011, 478(7370): 469–475
12 Varotsos C A, Crachnell A P, Tzanis C. The exceptional ozone depletion over the Arctic in January-March 2011. Remote Sens Lett, 2012, 3(4): 343–352
13 Adams C, Strong K, Zhao X, et al. Severe 2011 ozone depletion assessed with 11 years of ozone, NO_2, and OClO measurements at 80°N. Geophys Res Lett, 2012, 39(5): L05806
14 Randel W J, Wu F. Cooling of the Arctic and Antarctic polar stratospheres due to ozone depletion. J Climate, 1999, 12(5): 1467–1479
15 Rex M, Salawitch R J, Von Der Gathen P, et al. Arctic ozone loss and climate change. Geophys Res Lett, 2004, 31(4): L04116
16 Platt U. Differential optical absorption spectroscopy//Sigrist M W. Air monitoring by spectroscopic techniques. New York: Wiley and Sons. Inc, 1994: 27–84
17 Kim Y J, Platt U. Advanced environmental monitoring. Netherlands: Springer, 2008
18 Hönninger G, Von Friedeburg C, Platt U. Multi axis differential optical absorption spectroscopy (MAX-DOAS). Atmos Chem Phys, 2004, 4(1): 231–254
19 Fraser A, Adams C, Drummond J R, et al. The polar environment atmospheric research laboratory UV–visible ground-based spectrometer: First measurements of O_3, NO_2, BrO, and OClO columns. J Quant Spectrosc Radiat Transfer, 2009, 110(12): 986–1004
20 Frieß U, Kreher K, Johnson P V, et al. Ground-based DOAS measurements of stratospheric trace gases at two Antarctic stations during the 2002 ozone hole period. J Atmos Sci, 2005, 62(3): 765–777
21 Wittrock F, Oetjen H, Richter A, et al. MAX-DOAS measurements of atmospheric trace gases in Ny-Ålesund. Atmos Chem Phys, 2003, 3: 6109–6145
22 Luo Y H, Sun L G, Liu W Q, et al. MAX-DOAS measurements of NO_2 column densities and vertical distribution at Ny-Alesund, Arctic during summer. Spectrosc Spect Anal, 2012, 32(9): 2335–2340
23 Fayt C, Van Roozendael M. WinDOAS 2.1—software user manual. Belgium: Uccle, 2001
24 Rozanov A, Rozanov V, Burrows J P. A numerical radiative transfer model for a spherical planetary atmosphere: combined differential-integral approach involving the Picard iterative approximation. J Quant Spectrosc Rad Transfer, 2001, 69(4): 491–512
25 Gielen C, Van Roozendael M, Hendrik F, et al. Development of a cloud-screening method for MAX-DOAS measurements. EGU, 2013, 15, 7153G
26 Tzanis C. On the relationship between total ozone and temperature in the troposphere and the lower stratosphere. Int J Remote Sens, 2009, 30(23): 6075–6084